20th Australasian Fluid Mechanics Conference
Perth, Australia
5-8 December 2016

Estimation of Fluctuating Pressure Fields via Time-Mean Flow and Pointwise Measurements

F. Gómez[1], A. S. Sharma[2], and H. M. Blackburn[1]

[1]Department of Mechanical and Aerospace Engineering,
Monash University, VIC 3800, Australia

[2]Aerodynamics and Flight Mechanics,
University of Southampton, Southampton SO17 1BJ, UK

Abstract

A novel method to estimate pressure fields from pointwise velocity measurements is presented. As opposed to other existing methodologies, time-resolved full velocity fields are not required. The methodology is based on a resolvent-based reduced-order model which requires the mean flow to obtain physical flow structures and pointwise measurement to calibrate their amplitudes. The technique is applied to the unsteady flow around an square cylinder at low Reynolds number. The potential of the methodology is demonstrated through good agreement between the fluctuating pressure distribution on the cylinder and the temporal evolution of the unsteady lift coefficient predicted by the model and those computed by direct numerical simulation.

Introduction

Fluctuating pressure fields associated to unsteady separations and vortex shedding may lead to unsteady aerodynamic loads of concern in multiple engineering applications, such as flight mechanics, wind engineering, acoustics and dynamic aeroelasticity. The identification of unsteady aerodynamic coefficients is especially critical if new air vehicle configurations are tested or if the flight envelope is extended beyond traditional manoeuvres [3]. Unsteady aerodynamic models are derived either from wind tunnel testing or directly from flight test data because unsteady simulations of realistic configurations are likely to remain unaffordable [11]. Besides classical force balance instrumentation, non-intrusive strategies to estimate unsteady aerodynamic forces from particle image velocimetry (PIV) are also well-known [6]. These methods are based on combining experimental data with the governing equations in such a way that, provided with time-resolved velocity fields, a surface or volume integration of the Navier–Stokes equations can yield the pressure field, and hence the unsteady pressure forces. A limitation of the methodology is that three-dimensional time-resolved PIV is required to obtain three-dimensional velocity fields, and hence recover corresponding pressure fields.

In the present work we employ a methodology to estimate fluctuating pressure fields, and their associated unsteady aerodynamic forces, that is able to overcome the need for time-resolved three-dimensional velocity fields. Similarly to PIV-based approaches, the present methodology is also based on the combination of measurements with the Navier–Stokes equations. However, instead of employing three-dimensional time-resolved snapshots of the velocity, the inputs of the methodology are the time mean flow and point measurements of the velocity. (We note that the mean flow field can notionally also be obtained from experimental point measurements.) The use of the mean flow is motivated by the resolvent decomposition of McKeon & Sharma [8]. A Reynolds decomposition applied to the Navier–Stokes equations reveals that the unsteady motions are dominated by the properties of a resolvent operator depending on the mean flow and spatial derivatives. This resolvent operator acts a forcing-to-response transfer function at each temporal frequency, hence the mean flow restricts the possible unsteady motions that may exist in the flow. A singular value decomposition (SVD) of the resolvent operator typically reveals that, at each particular frequency, there is a dominant unsteady flow structure with amplification ratio greater than other possible motions.

The feasibility of employing these dominant motions as a basis for the creation of reduced-order models of the fluctuating velocity field was recently demonstrated by Gómez *et al.* [4] for flow in a rectangular lid-driven cavity. The present work expands on that theme to include the fluctuating pressure field, hence allowing estimation of fluctuating forces on an immersed body, and in addition employs a novel matrix-free time-stepping algorithm to estimate resolvent SVD modes, allowing them to be readily calculated in non-trivial flow domains. As for the method of Gómez *et al.* [4], amplitudes of resolvent modes used in the reduced-order model are calibrated using pointwise measurements of the velocity. The new methodology is applied to the estimation of fluctuating forces imposed by the flow around an square cylinder.

Description of the methodology

Figure 1 illustrates schematically the construction of the model employed to estimate the unsteady forces. The time mean flow $\mathbf{u}_0(\mathbf{x})$ and a pointwise measurement $\mathbf{u}(\mathbf{x}_0,t)$ of the velocity history are the inputs, corresponding to the leftmost blocks. In principle, mean flow and probe information could be obtained independently either from experiments or simulations. A spectral analysis of the probe signal $\mathbf{u}(\mathbf{x}_0,t)$ identifies the active frequencies ω_i to be explored in the resolvent analysis of the mean flow. The dominant resolvent modes $\psi_{\omega_i,1}$ arising from the resolvent analysis corresponding to the active frequencies are calibrated with the probe signal to obtain the amplitudes coefficients $a_{\omega_i,1}$. A linear combination of the weighted resolvent modes then provides an approximation of the fluctuating velocity and associated pressure fields.

Resolvent decomposition

We follow a similar derivation of the resolvent decomposition as that proposed by [7]. This derivation differs from that by [4] in that the pressure is explicitly taken into account, instead of projecting the velocity onto a divergence-free basis. A Reynolds decomposition is applied to the total velocity $\hat{\mathbf{u}}(\mathbf{x},t) = \mathbf{u}_0(\mathbf{x}) + \mathbf{u}(\mathbf{x},t)$, with $\mathbf{u}(\mathbf{x},t)$ being the fluctuating velocity which may be decomposed as a sum of temporal Fourier modes

$$\mathbf{u}(\mathbf{x},t) = \sum_i \mathbf{u}_{\omega_i}(\mathbf{x}) \mathrm{e}^{-\mathrm{i}\omega_i t} \,. \tag{1}$$

The flow is assumed to be statistically steady thus the frequencies ω_i are real. A similar decomposition may be applied to the nonlinear terms, leading to $\mathbf{f}_{\omega_i} = -(\mathbf{u}\cdot\nabla\mathbf{u})_{\omega_i}$. These decompositions lead to a formulation of the Navier–Stokes equations

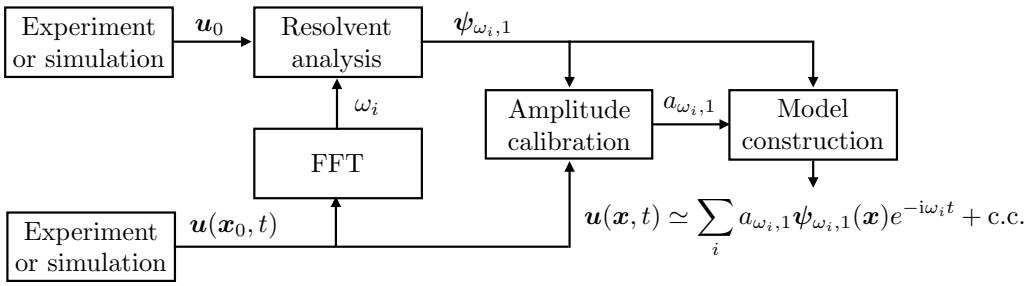

Figure 1: Diagram of the construction of the model. The mean flow and pointwise measurement inputs are on the leftmost blocks. A fast Fourier transform (FFT) of the probe signal provides the active frequencies ω_i to be explored in the resolvent analysis of the mean flow. The dominant resolvent modes $\psi_{\omega_i,1}$ corresponding to the active frequencies are calibrated with the probe signal to obtain the amplitudes coefficients $a_{\omega_i,1}$. A linear combination of the weighted resolvent modes provides an approximation of the fluctuating velocity and pressure. The fluctuating pressure is included in the fluctuating velocity vector $\mathbf{u} = (u,v,w,p)^{\mathrm{T}}$ for convenience.

as

$$\mathbf{u}_0\cdot\nabla\mathbf{u}_0 = -\nabla p + Re^{-1}\nabla^2\mathbf{u}_0 + \mathbf{f}_0 \quad (2)$$

$$\mathbf{u}_{\omega_i} = \mathcal{H}_{\omega_i}\mathbf{f}_{\omega_i}\,, \quad (3)$$

with $\mathcal{H}_{\omega_i}$ being the resolvent operator of the Navier–Stokes for each frequency ω_i. The mean flow equation (2) corresponds to $\omega = 0$ and Reynolds stress $\mathbf{f}_0$ denotes the interaction of the fluctuating velocity with the mean. The fluctuating pressure augments the fluctuating velocity vector as $\mathbf{u} = (u,v,w,p)^{\mathrm{T}}$ so the resolvent operator imposes the continuity equation

$$\mathcal{H}_\omega = \left(-\mathrm{i}\omega\begin{bmatrix} I & 0 \\ 0 & 0 \end{bmatrix} - \begin{bmatrix} \mathcal{L} & -\nabla \\ \nabla^{\mathrm{T}} & 0 \end{bmatrix}\right)^{-1}\begin{bmatrix} I & 0 \\ 0 & 0 \end{bmatrix}, \quad (4)$$

with $\mathcal{L}$ being the Jacobian of the Navier–Stokes equations and I an identity matrix. This operator represents how the fluctuating velocity $\mathbf{u}_\omega$ is driven by nonlinearity $\mathbf{f}_\omega$ in Fourier space, hence it is useful to inspect its amplification properties via a singular value decomposition (SVD)

$$\mathcal{H}_\omega = \sum_m \psi_{\omega,m}\sigma_{\omega,m}\phi^*_{\omega,m}\,, \quad (5)$$

where $\psi_{\omega,m}$ and $\phi_{\omega,m}$ are two orthonormal basis termed response and forcing modes respectively. The superscript $*$ indicates conjugate transpose and the subscript m indicates the ordering of the modes, ranked by the amplification given by the corresponding singular value $\sigma_{\omega,m}$ under the L_2 energy norm. The key of the resolvent decomposition is the projection on the nonlinearity onto the forcing modes [8], hence the fluctuating velocity can be written as a linear combination of response modes

$$\mathbf{u}_\omega = \sum_m \psi_{\omega,m}\sigma_{\omega,m}\chi_{\omega,m}\,, \quad (6)$$

where the unknown scalar coefficients $\chi_{\omega,m}$ are the projection of nonlinearity onto forcing modes and represent the forcing driving the velocity fluctuations [4].

Equation (6) is an exact representation of the Navier–Stokes equation because no assumption other than a statistically steady flow has been used. On the other hand, it is useful to exploit the values taken by the amplification $\sigma_{\omega,m}$ in order to construct a reduced-order model of the fluctuating velocity. In presence of a single dominant flow feature such as a centrifugal instability [4] or a critical layer response [8], the first singular value $\sigma_{\omega,1}$ is usually much larger than the second one $\sigma_{\omega,2}$, hence, at a particular frequency ω_i, irrespective of the values taken by $\chi_{\omega,m}$, it can be assumed that the projection of nonlinearity onto the first response $\psi_{\omega,1}$ is much larger than onto the rest. As such, the low-rank properties of the resolvent operator can be employed to yield a rank-1 model

$$\mathbf{u}_\omega \simeq \psi_{\omega,1}a_{\omega,1}\,, \quad (7)$$

where the amplitude coefficients $a_{\omega,1} = \sigma_{\omega,1}\chi_{\omega,1}$ represent the amount of nonlinearity being amplified. Under this rank-1 assumption, the fluctuating velocity (and pressure) can be expressed as

$$\mathbf{u}(\mathbf{x},t) \simeq \sum_\omega a_{\omega,1}\psi_{\omega,1}(\mathbf{x})\mathrm{e}^{-\mathrm{i}\omega t}\,, \quad (8)$$

hence this assumption provides a convenient model in which the velocity fluctuations at each frequency are parallel to the first singular response mode corresponding to that frequency. This rank-1 assumption has proven to be adequate in previous investigations of pipe, channel and cavity flows [8, 4].

Amplitude calibration

Obtaining resolvent modes $\psi_{\omega,1}$ can be computationally challenging in complex three-dimensional geometries even using time-stepping methods. However, only a small number of modes corresponding to the relevant or active frequencies in the flow are computed in practice. In the absence of further information, the active frequencies of the flow are identified via a Fourier analysis of a pointwise measurement of the flow. As highlighted in figure 1, the probe information can be obtained independently of the mean flow. Here we provide an extension of the calibration method developed by [4] to obtain the unknown amplitude coefficients that close the model (8) by using directly the same pointwise measurements of the velocity that have been previously employed for the identification of the active frequencies. At a particular spatial location $\mathbf{x}_0$, the reduced order model of the fluctuating velocity satisfies

$$\mathbf{u}(\mathbf{x}_0,t) \simeq \sum_{i=1}^{N_\omega}\psi_{\omega_i,1}(\mathbf{x}_0)a_{\omega_i,1}\mathrm{e}^{-\mathrm{i}\omega_i t}\,. \quad (9)$$

with N_ω representing the number of active frequencies (or discretized frequency bins) of the flow. Although each scalar component of (9) contains N_ω unknowns, it can be evaluated at a number of different time instants $N_t > N_\omega$, such that the solution is amenable to a least-squares approximation. We note that the spatial structure of the fluctuating velocity is restricted by the response modes, hence the pointwise calibration of the amplitude coefficients serves to capture the temporal behaviour of

the fluctuating velocity. The solution of (9) in a least-squares sense is given by

$$\mathcal{A} = \Psi^{+}\,\mathcal{U}(\mathbf{x_0},t) \tag{10}$$

with the $3N_t \times N_\omega$ matrix Ψ containing the values of the three velocity components of the resolvent modes and their complex conjugates at the spatial location $\mathbf{x}_0$ at N_t different times, the $N_\omega \times 1$ vector $\mathcal{A}$ representing the unknown amplitude coefficients, and the $3N_t \times 1$ vector $\mathcal{U}$ contains the values of the velocity at the spatial location $\mathbf{x}_0$ at different times. The superscript $+$ denotes pseudo-inverse. The dimensions of the least-squares problem (10) are much smaller than that of the SVD computations and its solution is straightforward. Finally, the least-squares method employed to fit the amplitudes is optimal in minimizing the variance. Hence in the case of Gaussian noise, the method would lead to a zero mean error. As such, sensor noise in the measurements would not be an issue for the present method.

Obtaining resolvent modes using time-stepping

The most computationally demanding step in the creation of the model, depicted in figure 1, is obtaining the resolvent modes. As such, efficient methods to evaluate the resolvent operator are essential for the feasibility of the present methodology for the estimation of aerodynamic forces. We note from equation 4 that the resolvent operator can be evaluated via a shift and inversion of the Jacobian, hence matrix-free or matrix-forming methods, typically employed for global stability analysis [10], can be used to study the resolvent operator.

Although the simplest way to obtain numerically the resolvent modes is to assemble the resolvent operator and perform a SVD, this is difficult in practice owing to the massive computational requirements resulting from the large dimensionality of the operator associated to flows with three non-homogeneous spatial directions. Thus matrix-free methods are preferred for the study of these flows. In what follows, we have employed the matrix-free time-stepping methodology described by Gómez *et al.* [5] to obtain the resolvent modes.

Application to the flow around an square cylinder

The flow past a two-dimensional square cylinder may serve as a model for the flow around a non-trivial bluff body and it is a good compromise between computational affordability and complex flow features [6]. Beyond the critical Reynolds number, the wake becomes unsteady presenting asymmetric vortex shedding, thus this flow is interesting for the investigation of unsteady lift and drag forces.

Although the present methodology seems more appealing for experimental works, the mean flow and pointwise measure inputs to the model have been obtained via direct numerical simulation (DNS) using a spectral-element solver [2]. A rectangular computational domain defined in $[-16,20]\times[-14,14]$ has been discretized with 236 spectral elements. The square cylinder has a unit side length and its centroid is located at $(x,y) = (0,0)$. Temporal and spatial convergence has been achieved with a polynomial expansion of order 11 in each element and using a second-order temporal scheme with $\Delta t = 8.5\times10^{-3}$. A constant velocity $(u,v) = (1,0)$ is imposed at the inlet of the domain, no-slip boundary condition at the cylinder wall and Neumann boundary conditions are imposed at the outlet. The Reynolds number based on the cylinder side length D and the modulus of the inlet velocity is fixed to $Re = 100$.

The inputs to the model corresponding to the leftmost block in figure 1, mean flow and a single pointwise measurement of the velocity, have been obtained via DNS. The probe is located at a random point in the wake of the cylinder where the shear is non-zero and it serves to identify a single dominant frequency $\omega_1 = 0.91$, hence only one resolvent mode corresponding to that frequency needs to be computed. We anticipate that the dynamics of the self-interaction of this mode in this kind of flows may be relevant due to the flow symmetry [9] thus it is required to consider the first harmonic $\omega_2 = 2\omega_1$ to predict the fluctuating drag. However, only a single mode is required for flow domains without symmetries, e.g., an inclined square cylinder [5].

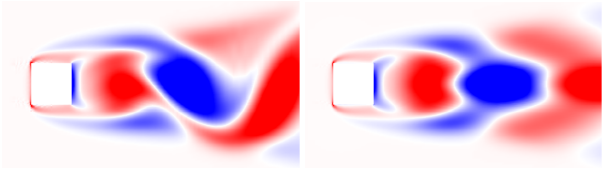

Figure 2: Comparison of the fluctuating vorticity fields obtained from (left) DNS and (right) resolvent-based model via calibration of the amplitude against probe data. Colored contours represent $\pm 1/3$ of the maximum and minimum vorticity.

The iterative time-stepping algorithm described by Gómez *et al.* [5] has been employed to obtain the two resolvent modes required to construct the reduced-order model. The forced linearized Navier–Stokes equations and their adjoint version have been solved with the same spectral-element solver employed for DNS. The boundary conditions for each equations are described by [1], however two set of boundary conditions at the inlet have been tested for the forced adjoint equations, (i) an extended domain $[-40,20]\times[-14,14]$ with Dirichlet boundary conditions and (ii) the same domain employed for the DNS with a non-physical forcing $-m(\mathbf{x})\mathbf{u}(\mathbf{x},t)$ applied at $-16 < x < 12$ to force a zero-amplitude of the forcing mode at $x = -16$. Both boundary conditions have provided similar results, thus the former has been adopted on account of smaller computational requirements.

A comparison of the vorticity fields obtained from DNS and the resolvent-based model via calibration of the amplitude against probe data is shown is figure 2. It is remarkable that flow in the region around the cylinder, and hence the unsteady separation, is accurately predicted by the model, despite the probe being located approximately three side lengths from the cylinder. On the other hand, the structure of the wake far from the cylinder present obvious discrepancies. Although the general feature of vortex shedding is also reproduced, the DNS presents additional features that the present resolvent-based mode does not capture, like a consecutive and opposite vertical displacement of the vortex cores. We presume that the additional dynamics of the far wake are governed by additional subdominant resolvent modes associated with the shear in the wake not considered in the present model.

The present approach is validated by measuring the unsteady lift coefficient defined as:

$$C_l' = \int_{\delta\Omega_c} p(\mathbf{x})\mathbf{n}\cdot\mathbf{e}_y, \tag{11}$$

where $\delta\Omega_c$ denotes the boundary of the cylinder, $\mathbf{n}$ is the normal vector around the square cylinder while $\mathbf{e}_y$ is the unit vector in the normal direction. At the present value of Re, the contributions of the viscous forces are negligible. Nevertheless, they could be taken into account using the present methodology. A good agreement between the temporal evolution of the unsteady lift coefficient calculated via DNS and predicted by the present methodology is shown in figure 3.

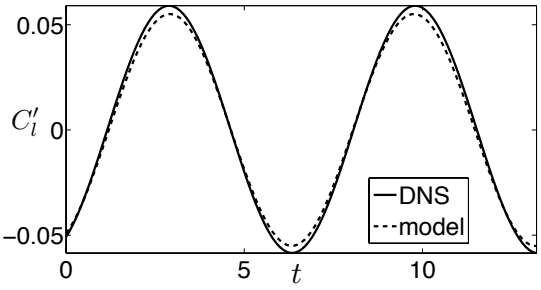

Figure 3: Comparison of the temporal evolution of the unsteady lift coefficient calculated via DNS and predicted by the present methodology.

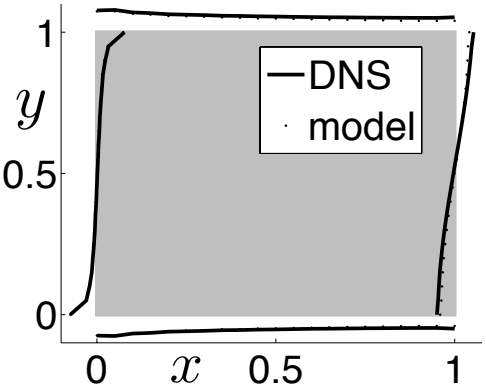

Figure 4: Representation of the fluctuating pressure distribution along the sides of the cylinder at a random instant calculated via DNS and predicted by the present methodology. Each cylinder side acts as a $x-$axis while their normal direction indicates the relative value of unsteady pressure at that location.

This results is consistent with the accurate prediction by the model of the near field around the cylinder shown in figure 2. To provide further insight, the fluctuating pressure distribution along the sides of the cylinder at a random instant is represented in figure 4. The resemblance between the pressure distributions corresponding to DNS and the resolvent-based model supports the good agreement between the temporal evolution of the unsteady lift force. Finally, the same approach has been carried out using different pointwise measurements. As remarked by [4], similar results have been obtained provided that the probe is always positioned at a location where the fluctuating velocity is significant. As such, care is needed in the selection of the probe locations, e.g., a probe far from the wake would present a negligible fluctuating velocity or a probe in the wake centerline far from the cylinder would only show dynamics corresponding to the first harmonic frequency ω_2. However, this potential pitfall can be easily overcome by selecting more than one probe location, as shown by [4]. Furthermore, the locations where the fluctuating velocity is significant can be inferred from the spatial structure of the resolvent modes.

Conclusions

A novel method to estimate unsteady aerodynamic coefficients via pointwise measurements has been presented. The methodology requires two inputs (i) the mean flow and (ii) temporal information from a probe. In principle, both inputs could be obtained either simultaneously or independently. Although we believe the present methodology is more appealing for experimental investigations, e.g. using planar time-resolved PIV to obtain a three-dimensional mean flow and obtain temporal information at different locations, DNS was employed in the present work to obtain the mean flow and the pointwise data.

The potential of the present methodology has been demonstrated by application to an unsteady two-dimensional flow around an square cylinder at low Reynolds number. The present approach can predict the fluctuating velocity associated with unsteady separation and the pressure distribution near the square cylinder using just the leading response mode. The temporal evolution of lift coefficient computed from those fields are in good agreement with those obtained via DNS.

Acknowledgements

The authors acknowledge financial support from the Australian Research Council through grant DP130103103, and from Australia's National Computational Infrastructure via Merit Allocation Scheme grant D77.

References

[1] Barkley, D., Blackburn, H. M. and Sherwin, S. J., Direct optimal growth analysis for timesteppers, *Int. J. Num. Meth. Fluids*, **57**, 2008, 1435–1458.

[2] Blackburn, H. M. and Sherwin, S. J., Formulation of a Galerkin spectral element–Fourier method for three-dimensional incompressible flows in cylindrical geometries, *J. Comput. Phys.*, **197**, 2004, 759–778.

[3] Brunton, S. L., Rowley, C. W. and Williams, D. R., Reduced-order unsteady aerodynamic models at low Reynolds numbers, *J. Fluid Mech.*, **724**, 2013, 203–233.

[4] Gómez, F., Blackburn, H. M., Rudman, M., Sharma, A. S. and McKeon, B. J., A reduced-order model of three-dimensional unsteady flow in a cavity based on the resolvent operator, *J. Fluid Mech.*, **798**, 2016, R2–1–14.

[5] Gómez, F., Sharma, A. S. and Blackburn, H. M., Estimation of unsteady aerodynamic forces using pointwise velocity data, *J. Fluid Mech.*, **802**, 2016, R4–1–12.

[6] Kurtulus, D. F., Scarano, F. and David, L., Unsteady aerodynamic forces estimation on a square cylinder by TR-PIV, *Exp. Fluids*, **42**, 2007, 185–196.

[7] Luhar, M., Sharma, A. S. and McKeon, B. J., Opposition control within the resolvent analysis framework, *J. Fluid Mech.*, **749**, 2014, 597–626.

[8] McKeon, B. J. and Sharma, A. S., A critical layer framework for turbulent pipe flow, *J. Fluid Mech.*, **658**, 2010, 336–382.

[9] Noack, B. R., Afanasiev, K., Morzyński, M., Tadmor, G. and Thiele, F., A hierarchy of low-dimensional models for the transient and post-transient cylinder wake, *J. Fluid Mech.*, **497**, 2003, 335–363.

[10] Paredes, P., Hermanns, M., Le Clainche, S. and Theofilis, V., Order 10^4 speedup in global linear instability analysis using matrix formation, *Comput. Methods Appl. M.*, **253**, 2013, 287–304.

[11] Spalart, P. R. and Venkatakrishnan, V., On the role and challenges of CFD in the aerospace industry, *The Aeronautical Journal*, **120**, 2016, 209–232.